

DESYNCHRONIZATION OF COUPLED OSCILLATORS USING CHAOS

G. Mykolaitis

Department of Physics
Vilnius Gediminas Technical University
Lithuania
gytis@pfi.lt

A. Petrovas

Department of Automation
Vilnius Gediminas Technical University
Lithuania
andrius.petrovas@el.vgtu.lt

A. Tamaševičius

Division of Electronics
Center for Physical Sciences and Technology
Lithuania
tamasev@pfi.lt

R. Stoop

Institute of Neuroinformatics
University of Zürich and ETHZ
Switzerland
ruedi@ini.phys.ethz.ch

Abstract

A technique for desynchronization of a network of FitzHugh–Nagumo type mean-field coupled spiking neurons is described. The coupled network is externally driven from a chaotic oscillator via the coupling node. Chaotic waveform resets the phase of the mean field and thus effectively decouples the individual oscillators. Hardware experiments have been performed using an electrical circuit consisting of three nonidentical FitzHugh–Nagumo oscillators.

Key words

Synchronization, FitzHugh–Nagumo oscillators, chaos.

1 Introduction

Synchronization phenomena are abundant in nature, science, engineering and social life [Pikovsky, Rosenblum and Kurths, 2003]. Dynamical systems in diverse areas, such as physics, chemistry, biology, and electronics exhibit a tendency to operate in synchrony. In some cases synchrony has rather contradictory impact. For example, synchrony in neuronal networks is very important for information processing within a brain area. However, too strong synchrony of firing neurons cause essential tremor and Parkinson's disease symptoms. A large number of *feedback* and *non-feedback* methods to avoid synchronization of coupled oscillators in general, and more specifically in neuronal arrays, have been described in literature, e.g. [Popovych, Hauptmann and Tass, 2005; Popovych, Hauptmann and Tass, 2006; Tass, 2007; Pyragas, Popovych and Tass, 2007; Kano and Kinoshita, 2009].

In this paper, we describe the desynchronizing a network of FitzHugh–Nagumo (FHN) coupled oscillators by means of a simple *non-feedback* technique. The method is an alternative to the very recently suggested remote virtual grounding *feedback* technique [Petrovas, Tamaševičius and Stoop, 2011].

2 Array of the FitzHugh–Nagumo oscillators

Block diagram of an array of coupled FHN oscillators and circuit diagram of an individual oscillator is shown in Fig. 1 and Fig. 2, respectively.

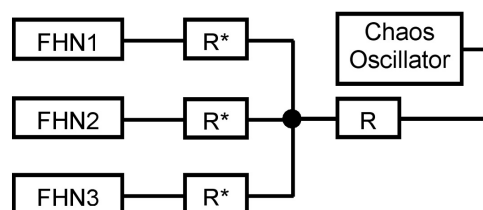


Figure 1. Block diagram of three mean-field coupled FHN oscillators with external chaos oscillator.

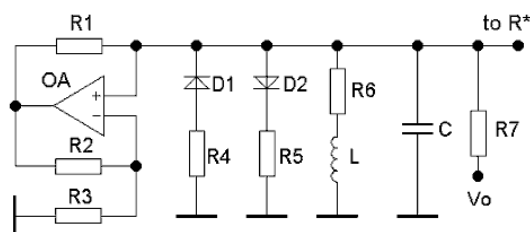


Figure 2. Circuit diagram of the FHN oscillator.

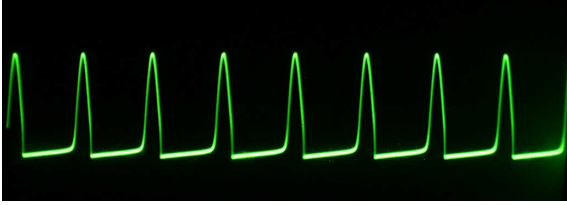


Figure 3. 5 ms length train of spikes from the FHN oscillator.

A single FHN oscillator has been described in detail elsewhere [Tamaševičiūtė *et al.*, 2009; Tamaševičius *et al.*, 2009]. Here, in Fig. 3 we present a typical train of spikes from the output of the circuit in Fig. 2, specifically from the node marked "to R*". The following circuit element values have been used in experiment: $R_1 = R_2 = 1 \text{ k}\Omega$, $R_3 = 560 \text{ }\Omega$, $R_4 = 30 \text{ }\Omega$, $R_5 = 470 \text{ }\Omega$, $R_6 = 220 \text{ }\Omega$, $R_7 = 47 \text{ k}\Omega$, $L = 100 \text{ mH}$, $C = 22 \text{ nF}$, $V_0 = -15 \text{ V}$.

3 Chaotic oscillator

Chaotic oscillator [Tamaševičiūtė, Mykolaitis and Tamaševičius, 2011] is depicted in Fig. 4 and is characterized by typical nonperiodic waveform and corresponding broadband continuous spectrum.

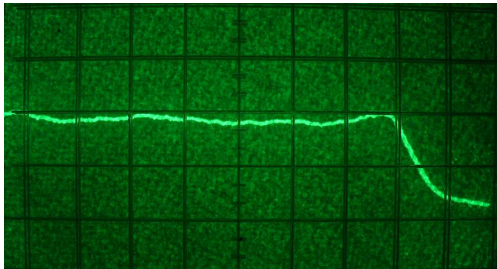
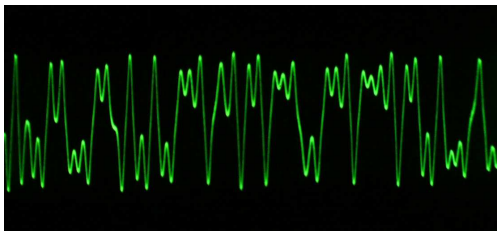
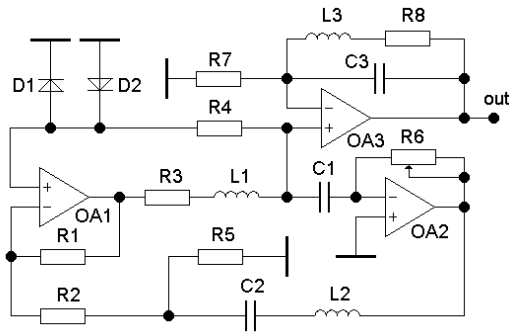


Figure 4. Chaotic oscillator. Top: circuit diagram. Middle: 10 ms length snapshot of chaotic waveform. Bottom: power spectrum in the range from 250 Hz to 5 kHz, vertical scale 10 dB/div., horizontal scale 0.5 kHz/div., resolution 100 Hz.

The following elements have been used to build the chaotic oscillator: $R_1 = R_2 = 20 \text{ k}\Omega$, $R_3 = R_8 = 62 \text{ }\Omega$, $R_4 = 68 \text{ k}\Omega$, $R_5 = 100 \text{ }\Omega$, $R_6 = 470 \text{ }\Omega$, $R_7 = 1.5 \text{ k}\Omega$, $L_1 = L_2 = 20 \text{ mH}$, $L_3 = 16 \text{ mH}$, $C_1 = 47 \text{ nF}$, $C_2 = 56 \text{ nF}$, $C_3 = 175 \text{ nF}$. The OA1, OA2 and OA3 are OP07 type operational amplifiers, the D1 and D2 are 1N4148 general-purpose diodes.

4 Non-synchronized FHN Oscillators

At large values of the coupling resistor R^* the all three oscillators, FHN1, FHN2, and FHN3 behave like isolated ones. They oscillate at their individual frequencies. We have intentionally set different inductance values in the individual oscillators, specifically $L_1 \approx 90 \text{ mH}$, $L_2 \approx 100 \text{ mH}$, and $L_3 \approx 110 \text{ mH}$ in FHN1, FHN2, and FHN3, respectively. Non-synchronized oscillators are illustrated with Lissajous figure, spectrum and time series in Fig. 5 for $R^* = 220 \text{ k}\Omega$.

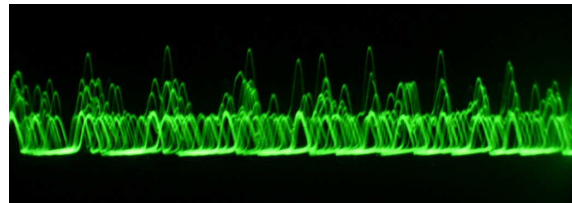
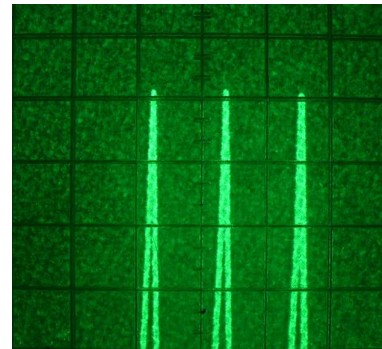
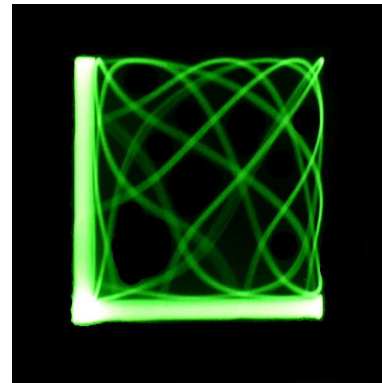


Figure 5. Non-synchronized FHN oscillators. Top: Lissajous figure (FHN1 versus FHN2). Middle: Spectrum of the voltage at the coupling node in the range from 1.2 to 1.8 kHz, vertical scale 10 dB/div., horizontal scale 100 Hz/div., resolution 3 Hz. Bottom: 5 ms length snapshot of the voltage at the coupling node.

5 Synchronized FHN Oscillators

With the decrease of the resistors R^* , that is with the increase of the coupling strength (the coupling coefficients can be estimated as $k_i = \sqrt{L_i/C}/R^*$, $i = 1, 2, 3$) the interaction between the individual oscillators becomes stronger. Eventually they appear phase locked. The results in Fig. 6 are presented for $R^* = 5.6 \text{ k}\Omega$. Though the oscillators have somewhat different phases as evident from the Lissajous figure in Fig. 6, they do oscillate at the same single frequency. In the previous section the array of oscillators exhibited three different incommensurate frequencies, namely $\approx 1.42 \text{ kHz}$, $\approx 1.53 \text{ kHz}$, and $\approx 1.65 \text{ kHz}$ (Fig. 5). Here we see a single line (higher harmonics are not shown) at $\approx 1.60 \text{ kHz}$ (Fig. 6). The waveform in Fig. 6 taken at the coupling node is very similar to the train of periodic spikes from a single uncoupled oscillator (Fig. 3). The only difference is that the width of the spikes is slightly larger due to the phase shift between the synchronized oscillators.

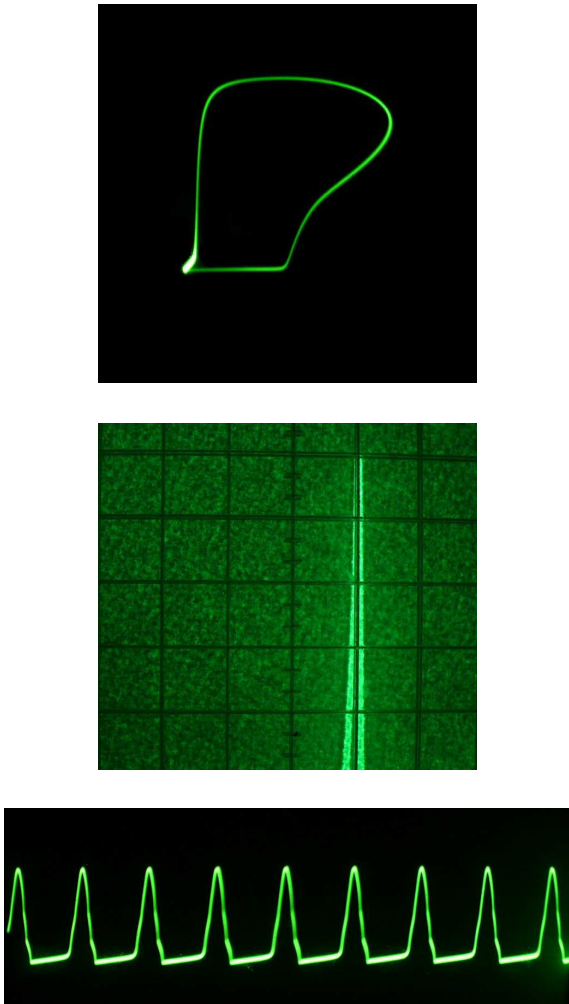


Figure 6. Synchronized FHN oscillators. Top: Lissajous figure (FHN1 versus FHN2). Middle: Spectrum of the voltage at the coupling node in the range from 1.2 to 1.8 kHz, vertical scale 10 dB/div., horizontal scale 100 Hz/div., resolution 3 Hz. Bottom: 5 ms length snapshot of the voltage at the coupling node.

6 Desynchronized FHN Oscillators

In this section we describe the influence of chaos on the synchronized FHN oscillators. Broadband signal from the chaos oscillator, characterized in section 3, is applied via the resistor $R \approx R^*$ to the coupling node. Frequency range of the chaotic signal (0 to 4 kHz) covers the first (1.6 kHz) and the second (3.2 kHz) harmonics of the mean field of the FHN oscillators. Therefore, chaos effectively disturbs the mean voltage $\langle V \rangle$ of the array and via the coupling resistors R^* effects the individual FHN oscillators. The control force is given by $k_i(\langle V \rangle - V_i)$, where V_i is the output voltage of an individual FHN oscillator. For sufficiently high level of chaos, e.g. $V_{ch} \approx 2 - 3 \text{ V}$, phase locking between the FHN oscillators is corrupted, as illustrated with Lissajous figure in Fig. 7. The continuous spectrum in Fig. 7 is localized near the individual frequencies of the FHN oscillators and occupies relatively narrow band. The waveform in Fig. 7 visually is similar to the waveform of non-synchronized oscillators (Fig. 5).

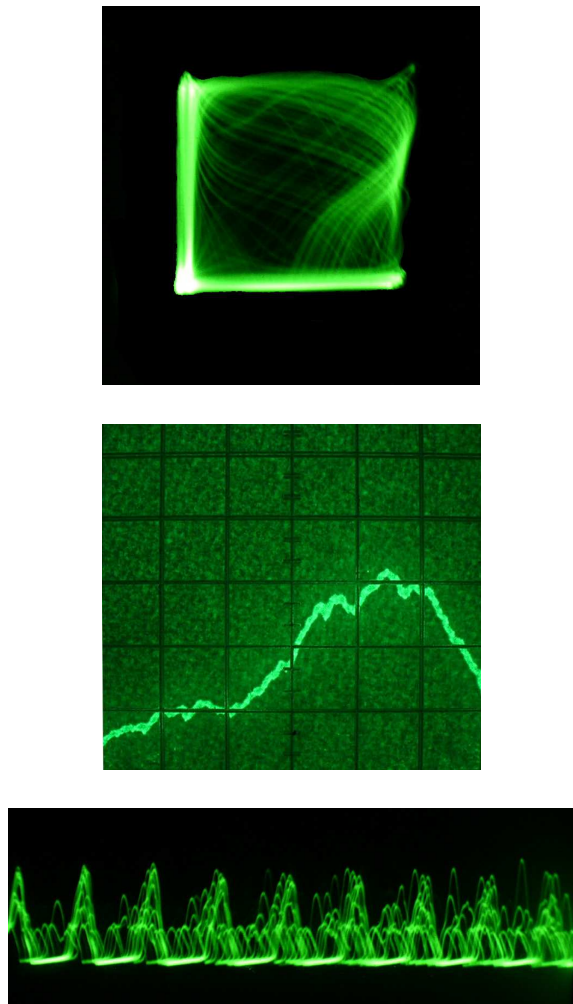


Figure 7. Desynchronized FHN oscillators. Top: Lissajous figure (FHN1 versus FHN2). Middle: Spectrum of the voltage at the coupling node in the range from 1.2 to 1.8 kHz, vertical scale 10 dB/div., horizontal scale 100 Hz/div., resolution 3 Hz. Bottom: 5 ms length snapshot of the voltage at the coupling node.

7 Desynchronization Using Noise

Intuitively one can argue that random noise is a good or even better alternative to chaos for desynchronization of coupled oscillators. Indeed, we have replaced the external chaotic oscillator with commercially available pseudorandom noise oscillator based on linear feedback shift registers. The employed noise oscillator is characterized by extremely flat spectral density of the output signal. The spectral unevenness is only 1 dB, i.e. much better than 3 dB for the chaotic oscillator (Fig. 3). Moreover, the upper limit of the spectral range of noise signal is 20 kHz (at -3 dB). Thus, noise signal covers all the 12 harmonics of the FHN oscillators (20 kHz/1.6 kHz \approx 12). By increasing the noise level we observed the same desynchronization phenomenon like using chaotic signals. The results for noise influence are not presented here, since all characteristics look the same as in Fig. 7. On the other hand chaotic oscillators are essentially simpler and cheaper than classical noise oscillators, especially at lower frequencies.

8 Concluding Remarks

We have built and investigated an experimental array of the FitzHugh–Nagumo type oscillators. The individual oscillators differ from the common FitzHugh–Nagumo electronic cells, e.g. [Binczak *et al.*, 2003; Aliaga *et al.*, 2003; Jacquir *et al.*, 2004; Jacquir *et al.*, 2006]. They contain asymmetric activation units as proposed in [Tamaševičiūtė *et al.*, 2009; Tamaševičius *et al.*, 2009]. We have demonstrated that the coupled oscillators can be desynchronized by applying chaotic signals to the coupling node. Chaos disturbs the mean field and consequently corrupts the phase locking between the oscillators. Investigations have been performed with relatively simple model, namely the FitzHugh–Nagumo type oscillators. We believe, however, that similar technique can be applied to networks composed of more sophisticated, e.g. the Hodgkin–Huxley neuron cells [Sitt and Aliaga, 2007].

Acknowledgement

One of us (A. P.) was supported under the postdoctoral fellowship being funded by European Union Structural Funds project Postdoctoral Fellowship Implementation in Lithuania within the framework of the Measure for Enhancing Mobility of Scholars and Other Researchers and the Promotion of Student Research VP1-3.1-ŠMM-01 of the Program of Human Resources Development Action Plan.

References

Aliaga, J., Busca, N., Mincev, V., Mindlin, G. B., Pando, B., Salles, A. and Sczupak L. (2003). Electronic Neuron within a Ganglion of a Leech (*Hirudo Medicinalis*). *Phys. Rev. E*, **67**, 061915.
Binczak, S., Kazantsev, V. B., Nekorkin, V. I. and Bilbaut, J. M. (2003). Experimental Study of Bifurca-

tions in Modified FitzHugh–Nagumo Cell. *Electron. Lett.*, **39**, pp. 961–962.
Jacquir, S., Binczak, S., Bilbaut, J. M., Kazantsev, V. B. and Nekorkin, V. I. (2004). Study of Electronic Master-Slave MFHN Neurons. In *Proc. 12th Int. Workshop on Nonlinear Dynamics of Electronic Systems*. Evora, Portugal, May, 9–13. pp. 182–185.
Jacquir, S., Binczak, S., Bilbaut, J. M., Kazantsev, V. B. and Nekorkin, V. I. (2006). Synaptic Coupling Between Two Electronic Neurons. *Nonlinear Dynamics*, **44**, pp. 29–36.
Kano, T. and Kinoshita S. (2009). Phase Control of Coupled Oscillators Using Multilinear Feedback. In *Proc. Int. Symp. Nonlinear Theory and its Applications*. Sapporo, Japan, Oct, 18–21. pp. 34–37.
Petrovas, A., Tamaševičius, A. and Stoop, R. (2011). Desynchronization of a network of FitzHugh–Nagumo Oscillators. *Electronics and Electrical Engineering*, in press.
Pikovsky, A., Rosenblum, M. and Kurths, J. (2003). *Synchronization: A Universal Concept in Nonlinear Sciences*. Cambridge University Press.
Popovych, O. V., Hauptmann, C. and Tass, P. A. (2005). Effective Desynchronization by Nonlinear Delayed Feedback. *Phys. Rev. Lett.*, **94**, 164102.
Popovych, O. V., Hauptmann, C. and Tass, P. A. (2006). Control of Neuronal Synchrony by Nonlinear Delayed Feedback. *Biol. Cyber.* **95**, pp. 69–85.
Pyragas, K., Popovych, O. V. and Tass, P. A. (2007). Controlling Synchrony in Oscillatory Networks with a Separate Stimulation–Registration Setup. *Eur. Phys. Lett.*, **80**, 40002.
Sitt, J. D. and Aliaga, J. (2007). Versatile Biologically Inspired Electronic Neuron. *Phys. Rev. E*. **76**, 051919.
Tamaševičius, A., Tamaševičiūtė, E., Mykolaitis, G., Bumelienė, S., Kirvaitis, R. and Stoop, R. (2009). Neural Spike Suppression by Adaptive Control of an Unknown Steady State. *Lecture Notes Comp. Sci.*, **5768**, pp. 618–627.
Tamaševičiūtė, E., Tamaševičius, A., Mykolaitis, G., Bumelienė, S., Kirvaitis, R. and Stoop, R. (2009). Electronic Analog of the FitzHugh–Nagumo Neuron Model and Noninvasive Control of its Steady State. In *Proc. 17th Int. Workshop on Nonlinear Dynamics of Electronic Systems*. Rapperswil, Switzerland, June, 21–24. pp. 138–141.
Tamaševičiūtė, E., Mykolaitis, G. and Tamaševičius, A. (2011). Autonomous Silva–Young Type Chaotic Oscillator with flat Power Spectrum. *Electronics and Electrical Engineering*, in press.
Tass, P. A. (2007). *Phase Resetting in Medicine and Biology: Stochastic Modelling and Data Analysis*. Springer. Berlin.